JOURNAL OF NANO- AND ELECTRONIC PHYSICS
Vol. **4** No 4, 04004(5pp) (2012)

ЖУРНАЛ НАНО- ТА ЕЛЕКТРОННОЇ ФІЗИКИ
Том **4** № 4, 04004(5cc) (2012)

Nonlinear Optical Rectification of Confined Exciton in a ZnO/ZnMgO Strained Quantum Dot

N.S. Minimala[1], A. John Peter[2]

[1] *Department of Physics, N.M.S. Sermathai Vasan College for Women, Madurai-625 012, India*
[2] *Department of Physics, Government Arts College, Melur-625 106. Madurai, India*

(Received 16 October 2012; revised manuscript received 22 October 2012; published online 29 December 2012)

Heavy hole exciton binding energies as functions of dot radius and the Mg alloy content in a ZnO/$Mg_xZn_{1-x}O$ quantum dot are investigated. The effects of strain, including the hydrostatic and the biaxial strain, and the internal electric field, due to spontaneous and piezoelectric polarization are taken into account. Numerical calculations are performed using variational procedure within the single band effective mass approximation. The nonlinear optical rectification is investigated for different dot radius and the values of Mg alloy content in a ZnO/$Mg_xZn_{1-x}O$ quantum dot taking into account the strain-induced piezoelectric effects. The results show that the resonant peak of the nonlinear optical rectification is blue shifted with the confinement effect and the Mg alloy content.

Keywords: Electronic states, Optical absorption, Quantum dot.

PACS numbers: 73.21.Fg, 42.65.An, 71.38. – k

1. INTRODUCTION

Blue and ultraviolet light emitters and detectors made from the wide band gap semiconductors are quite interesting. GaN ultraviolet diodes have been reported earlier [1, 2]. The best material to replace GaN is the ZnO based alloy semiconductor. ZnO based quantum nanostructures have several advantages over GaN semiconducting materials [3]. Lattice mismatch between the inner and outer material of ZnO is less compared to GaN material [4]. Doping ZnO with Cadmium or Magnesium will permit tailoring the band gap for some potential applications for hybrid optoelectronic devices.

Among II-VI wide band gap semiconductors, ZnO is interesting material for its potential applications in optoelectronic devices. Moreover, a large built-in internal fields due to spontaneous and piezoelectric polarizations exist in Wurtzite Mg based ZnO quantum wells [5]. Hence, it is a promising semiconductor with the direct band gap around 3.3 eV with some applications in short wavelength optical devices and long life time operating devices [6]. To understand the fundamental optical properties in opto-electronic devices, it is required to know the excitonic properties. ZnO has a larger exciton binding energy, around 60 meV [7]. The excitonic transition energy in ZnO/ZnMgO quantum wells has been reported for various well width earlier by theoretically [8] and experimentally [9]. The excitonic transition energy in ZnO/ZnMgO quantum wells has been studied with the inclusion of internal fields [10-12].

The ground-state donor binding energy of a hydrogenic impurity in wurtzite ZnO/MgZnO strained coupled quantum dots has been calculated using a variational method, considering the strong built-in electric field due to spontaneous and piezoelectric polarizations [13]. The nonlinear optical properties in low dimensional semiconductors are more pronounced than in bulk materials due to the quantum confinement effect [14, 15]. The nonlinear optical rectification in the asymmetric quantum well was studied earlier [16].

In the present paper, exciton binding energies of a heavy hole in a ZnO/$Mg_xZn_{1-x}O$ quantum dot are investigated with the geometrical confinement and the Mg alloy content. The effects of strain, including the hydrostatic and the biaxial strain, and the internal electric field, including the spontaneous and piezoelectric polarization are considered in all the calculations. Numerical calculations are performed using variational procedure within the single band effective mass approximation. The nonlinear optical rectification as functions of dot radius and the values of Mg alloy content is investigated in the strained ZnO/$Mg_xZn_{1-x}O$ quantum dot. In Section 2, we briefly describe the method and the model used in our calculations of obtained eigen functions and eigen energies of exciton states, interband emission energy and the linear and non-linear optical rectification coefficients. The results and discussion are presented in Section 3. A brief summary and results are presented in the last Section.

2. MODEL AND CALCULATIONS

Let us consider a Hamiltonian of a confined exciton, within the framework of single band effective mass approximation, in a cylindrical wurtzite ZnO/$Zn_{1-x}Mg_xO$ quantum dot which is characterized with its radius R and length L. The exciton consisting a single electron part (H_e), the single hole part (H_h) and Coulomb interaction term between electron-hole pair is given by,

$$\hat{H}_{exe} = H_e(\bar{r}_e) + H(\bar{r}_h) - \frac{e^2}{\varepsilon\left|\bar{r}_e - \bar{r}_h\right|} \qquad (1)$$

where, e is the absolute value of electron charge, $\left|\bar{r}_e - \bar{r}_h\right|$ denotes the relative distance between the electron and the hole and $\varepsilon = 8.4$ is the dielectric constant of ZnO material.

The Hamiltonian of the exciton in the strained ZnO/$Zn_{1-x}Mg_xO$ quantum dot can be written as,

$$H_{exc} = -\frac{\hbar^2}{2\mu_{\|}}\left[\frac{1}{\rho_j}\frac{\partial}{\partial\rho_j}\left(\rho_j\frac{\partial}{\partial\rho_j}\right)+\frac{1}{\rho_j^2}\frac{\partial^2}{\partial\varphi_j^2}\right]-\frac{\hbar^2}{2m_e^*}\frac{\partial^2}{\partial z^2}-\frac{\hbar^2}{2m_{h\perp}^*}\frac{\partial^2}{\partial z^2}+V(\rho,z_j)\pm eFz_j-\frac{e^2}{\varepsilon|r_e-r_h|} \quad (2)$$

where $j = e$ and h refer to the electron and hole, respectively, ε is the dielectric constant for the material inside the quantum dot, $V(\rho, z_j)$ is the confinement potential due to the contribution from the Mg dependent strain effect ($V_{c(v)strain}$) and the barrier offset. The sign + for the electron and – for hole with F is the built-in internal field due to the spontaneous and piezoelectric polarizations in the wurtzite ZnO / ZnMgO quantum structure. The reduced mass in the x-y plane is given by

$$\mu_{\|} = \frac{m_e m_{h\|}}{m_e + m_{h\|}}. \quad (3)$$

Assuming the mass of the electron as isotropic and hence $m_{e\|}^* = m_{e\perp}^* = m_e^*$. The hole masses are determined from the Luttinger parameters γ_1 and γ_2 which are expressed as [17]

$$\frac{1}{m_{h\perp}} = \frac{1}{m_0}(\gamma_1 - 2\gamma_2) \quad (4)$$

$$\frac{1}{m_{h\|}} = \frac{1}{m_0}(\gamma_1 + \gamma_2) \quad (5)$$

where, m_0 is the free electron mass.

The energy shifts of the strained conduction band and valence band are calculated below. The strain-induced potential for the conduction band in the influence of Mg- incorporation is given by [18]

$$V_{Cstrian}(x) = a_c[\varepsilon_{xx}(x) + \varepsilon_{yy}(x) + \varepsilon_{zz}(x)] \quad (6)$$

where, a_c is the deformation potential constant of conduction band, $\varepsilon_{xx}(x) = \varepsilon_{yy}(x) = 1 - a(x)/a_0(x)$ where $a_0(x)$ and $a(x)$ are the Mg-dependent lattice parameters of bulk ZnO (0.567 nm) and MgO (0.591 nm) respectively. The change in length is occurred as the ZnO has a smaller bond length than MgO. And $\varepsilon_{zz}(x) = -2C_{12}(x)\varepsilon_{xx}(x)/C_{11}(x)$, the values of parameters $C_{11}(x)$ and $C_{12}(x)$ are shown in Table 1.

The strain-induced potential for the valence band with the incorporation of Mg in ZnO which can be written as [19]

$$V_{Vstrain}(x) = a_v[(\varepsilon_{xx}(x) + \varepsilon_{yy}(x) + \varepsilon_{zz}(x)) - -\frac{b}{2}(\varepsilon_{xx}(x) + \varepsilon_{yy}(x) - 2\varepsilon_{zz}(x)] \quad (7)$$

where a_v and b are the deformation potential constants of valence band.

The electron (hole) confinement potential, $V(\rho, z_j)$, due to the band offset in the ZnO/ $Zn_{1-x}Mg_xO$ quantum dot structure is given by

$$V(\rho,z) = \begin{cases} V_I(\rho) & -\frac{L}{2} \le z \le \frac{L}{2} \\ V_{II} & |z| > \frac{L}{2} \end{cases} \quad (8)$$

$$V(\rho) = \begin{cases} 0 & \rho \le R \\ V_0 & \rho > R \end{cases} \quad (9)$$

where, L is the height of the cylindrical quantum dot, R is the dot radius and V_0 is expressed as

$$V_0 = Q_c\Delta E_g \quad (10)$$

where, Q_c is the conduction band offset parameter which is taken as 60 : 40 between conduction band and valence band [20] and the ΔE_g is the band gap of ZnO.

Thus, the total strain induced band gap is given by

$$E_g(x) = E_g + \delta E_{HH}(x) \quad (11)$$

with

$$\delta E_{HH}(x) = \frac{1}{3}\Delta_0 - a_c - a_v\left(\frac{2C_{12}(x)}{C_{11}(x)+C_{12}(x)}+2\right)\times \times\left(\frac{a_0(x)-a(x)}{a(x)}\right) \quad (12)$$

The polarization in a self-formed wurzite quantum dot has both a spontaneous and a piezoelectric component. The piezoelectric tensor will have three independent nonvanishing components (e31, e33, e15) [21]. Thus the total polarization, $\vec{P}_{tot}$ is sum of the spontaneous polarization $\vec{P}_{SP}$ and the piezoelectric polarization $\vec{P}_{PE}$ without the external electric field.

The direction of the built-in electric field F depends on the orientation of the piezoelectricity and spontaneous polarization In this case, the direction of the piezoelectricity and spontaneous polarization is along the z direction [22].

$$P_{Zn_{1-x}Mg_xO}^{SP}(x) = -(0.057 + 0.66x)\ C/m^2 \quad (13)$$

The stress induced piezo electric field (P^{PZ}) related to mismatch between the dot and the barrier material along the z-direction is given by

$$P^{PZ}(x) = e_{31}(x)(\varepsilon_{xx}(x) + \varepsilon_{yy}(x)) + e_{33}(x)\varepsilon_{zz}(x) \quad (14)$$

where $\varepsilon_{xx}(x), \varepsilon_{yy}(x)$ and $\varepsilon_{zz}(x)$ are the strain elements in $Zn_{1-x}Mg_xO$ layers as defined earlier. Thus the piezoelectric polarization is given by

$$P^{PZ}(x) = 2\varepsilon_{xx}(x)\left(e_{31}(x) - \varepsilon_{33}(x)\frac{C_{13}(x)}{C_{33}(x)}\right) \quad (15)$$

where e_{ij} is the piezoelectric constants. Thus the total electric fields within the quantum dot and the barrier are given by [23]

$$F_{dot} = \left|-\frac{(P_{SP(\mathrm{ZnO})} + P_{PE(\mathrm{ZnO})} - P_{SP(\mathrm{ZnMgO})})L_{(\mathrm{ZnMgO})}}{\varepsilon_0(2\varepsilon_{e(\mathrm{MgZnO})}L_{(\mathrm{ZnO})} + \varepsilon_{e(\mathrm{ZnO})}L_{(\mathrm{ZnMgO})})}\right| \quad (16)$$

$$F_{barrier} = 2\left|\frac{(P_{SP(\mathrm{ZnO})} + P_{PE(\mathrm{ZnO})} - P_{SP(\mathrm{ZnMgO})})L_{(\mathrm{ZnO})}}{\varepsilon_0(2\varepsilon_{e(\mathrm{ZnMgO})}L_{(\mathrm{ZnO})} + \varepsilon_{e(\mathrm{ZnO})}L_{(\mathrm{ZnMgO})})}\right| \quad (17)$$

where, ε_0 is the dielectric constant of the respective material. Here, ε_e is the electronic dielectric constant of material, P_{SPZnO}, P_{PEZnO}, and P_{SPZnMgO} are the spontaneous polarizations and piezoelectric polarizations of ZnO and the spontaneous polarization of ZnMgO respectively. The above values can be generally calculated by the polarity of the crystal and the strains of the quantum nanostructure. Since the wurtzite crystal lattice of ZnO and MgO lack inversion symmetry, the heterostructure will have spontaneous polarization (P_{SP}) and the piezo electric polarization (P_{PZ}) due to strain caused by the lattice mismatch between ZnO and MgO material.

We have chosen the trial wave function for the exciton ground state, within the variational scheme. We take the problem of an exciton in a ZnO/$Zn_{1-x}Mg_xO$ quantum dot within the single band effective mass approximation, it is necessary to use a variational approach to calculate the eigen function and eigen value of the Hamiltonian and to calculate the bound exciton ground state energy. Considering the correlation of the electron-hole relative motion, the trial wave function can be chosen as,

$$\Psi(\bar{r}_e, \bar{r}_h) = f_e(z_e)f_h(z_h)e^{-\alpha\rho^2}e^{-\beta z^2} \quad (18)$$

where, f_e and f_h are ground state solution of the Schrödinger equation for the electrons and holes in the absence of the Coulomb interaction, given by

$$f_e(z_e) = \begin{cases} \cos(k_e z_e) & z_e \le |L/2| \\ A_e \exp(-\delta_e |z_e|) & z_e > |L/2| \end{cases} \quad (19)$$

$$f_h(z_h) = \begin{cases} \cos(k_h z_h) & z_h \le |L/2| \\ A_h \exp(-\delta_h |z_h|) & z_h > |L/2| \end{cases} \quad (20)$$

The Eq. (18) describes the correlation of the electron-hole relative motion. α and β are variational parameters responsible for the in-plane correlation and the correlation of the relative motion in the z-direction respectively [24]. By matching the wave functions and the effective mass and their derivatives at boundaries of the quantum dot and along with the normalization, we fix all the constants (A_e, A_h, δ_e, δ_h, k_e and k_h) except the variational parameters. These constants are obtained by the interface conditions between the dot and the barrier. So the wave function Eq. (18) completely describes the correlation of the electron-hole relative motion.

The Schrödinger equation is solved variationally by finding $\langle H \rangle_{min}$ and the binding energy of the exciton in the quantum dot is given by the difference between the energy with and without Coulomb term. First, we concentrate on the calculation of the electronic structure of the ZnO / ZnMgO quantum dot system for various Mg alloy content by calculating its subband energy (E) and subsequently the exciton binding energy. To calculate the ground-state energies of the heavy excitons, we minimize the expectation values of the Hamiltonian (Eq. (1)) calculated using a trial function with two variational parameters (Eq. (18)). Then, by using the density matrix approach, within a two-level system approach, the explicit expression for the nonlinear optical properties such as the nonlinear optical rectification is computed in saturation limit. The dependence of the nonlinear optical processes on the dot sizes is investigated with the different photon energy.

The binding energy of the excitonic system is defined as

$$E_{exc}(x) = E_e + E_h - \langle H_{exc} \rangle_{\min} \quad (21)$$

where, $E_{e,h}$ is the sum of the free electron and the free hole self-energies in the same quantum dot. The second order nonlinear optical rectification coefficient is given by [25, 26]

$$\chi_0^2 = \frac{q^3\sigma_s\mu_{01}^2\delta_{01}}{\varepsilon_0} \frac{2\Delta E^2}{\left[(\Delta E - \hbar\omega)^2 + (\hbar\Gamma_0)^2\right]\left[(\Delta E + \hbar\omega)^2 + (\hbar\Gamma_0)^2\right]} \quad (22)$$

where σ_s is the electron density in the quantum dot, ε_0 is the vacuum permittivity, $\Gamma = 1/\tau$ is the relaxation rate for states 1 and 2 and $\hbar\omega$ is the photon energy. The Matrix element, $\mu_{01} = \langle \psi_0 | z | \psi_1 \rangle$ is defined as the electric dipole moment of the transition from the ground state (ψ_0) to the first excited state ψ_1 with $\delta_{01} = \langle \psi_1 | z | \psi_1 \rangle - \langle \psi_0 | z | \psi_0 \rangle$. ΔE is the absorption energy from ψ_0 to ψ_1. We have taken the relaxation rate as 1 ps and the electron density is taken as 1×10^{24} m^{-3}.

3. RESULTS AND DISCUSSION

The exciton binding energy is computed numerically and thereby nonlinear optical property is discussed in the cylindrical ZnO / $Zn_{1-x}Mg_xO$ strained quantum dot, for various Mg alloy content, with the heavy hole mass as the heavy excitons are more common in experimental results. The nonlinear optical properties such as nonlinear optical rectification as a function of photon energy for different Mg concentration ($x < 0.3$) in ZnO / $Zn_{1-x}Mg_xO$ quantum dot are investigated. Since $Mg_xZn_{1-x}O$ remains in a hexagonal phase wurtzite crystal with the ZnO, up to Mg alloy content (0.33) [27] we have limited our case upto 0.3 and hence Mg based ZnO material can be realized a perfect lattice matched material with an appropriate combination of magnesium concentration in ZnO material. And also, we bring out the effects of built-in electric field, due to piezoelectric polarization and the spontaneous polarization for different Mg content. The material parameters used in this study are tabulated in Table 1.

We present the variation of exciton binding energy as a function of dot radius of a ZnO / $Zn_{1-x}Mg_xO$ single quantum dot for various Mg alloy content (solid line) and without (dashed curve) the internal field due to polarization effect in Fig. 1. In all the cases, it is observed that the exciton binding energy increases with a decrease of dot radius, reaching a maximum value and

Table 1 – Material parameters for ZnO, MgO and other values of Zn1 – *x*Mg*x*O (linearly interpolated from the data of ZnO and MgO) used in the calculations

Parameter	ZnO	MgO
E_g (eV)	3.25	5.29
A (nm)	0.567	0.591
e_{31} (c/m^2)	– 0.57	– 0.38
e_{33} (c/m^2)	1.34	2.26
C_{11} (GPa)	209.7	222
C_{12} (GPa)	121.1	90
C_{13}	10.51	5.8
C_{33}	21.09	10.9
a_v (eV)	– 0.6	2.0
a_c (eV)	– 2.3	– 4.3
Piezo electric constants	8.1	9.8
Piezo electric constants (C/m^2)	– 5.0	– 6.32

Parameters are taken from the Ref.[30, 31].

then decreases when the dot radius still decreases. It is because an increase in the dot radius results in a spreading of the wave function which causes the lowering in the binding energy. Variation in Mg composition causes the change in the barrier height of the quantum dot. As the dot radius approaches zero the confinement becomes negligibly small, and in the finite barrier problem the tunnelling becomes huge eventually the penetration of the exciton wave function in the barriers dominates. This results in the decrease in the binding energy as the dot radius becomes small. Our results are in good agreement with the previous investigator [28]. The large exciton binding energy implies that the excitons play an important role in the linear and the non-linear optical response of Mg based ZnO quantum nanostructures. The exciton confinement increases with the Mg composition. The enhancement of exciton energy with the reduction of dot radius is due to the spatial confinement. The inclusion of internal field due to the strain-induced piezoelectric effects reduces the exciton binding energy. Thus, the results indicate that any quantum device depends on the composition of the barrier material and the spatial confinement of dot size.

Fig. 2 shows the variation of second order nonlinear coefficient as a function of incident energy for a confined exciton for various Mg alloy content in a 70 Å ZnO / $Zn_{1-x}Mg_xO$ quantum dot.It is found that the resonant peak is blue shifted as the Mg alloy content increases in the barrier. It is known that the exciton binding energy increases with the Mg concentration in the barrier. It is because the barrier height increases with the Mg alloy content. The magnitude of the resonant peak of nonlinear optical rectification is found to be around 10^{-4} m/V. This strength of nonlinear optical rectification matches with the other wide band gap semiconductors [29]. This strong value is due to the existence of larger dipole matrix elements in the wide band gap semiconductors.

Here, we observe that the variation of magnitude of rectification coefficient decreases with decreasing dot radius. The spacing between the energy levels increases due to decrease in dot radius. It is because the exciton binding energy decreases when the dot radius is increased. Thus, the resonant frequencies are important and it should be taken into account in studying the optical properties of exciton in the quantum nanostructures.

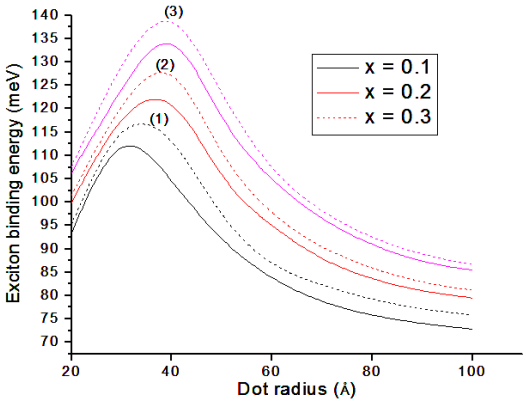

Fig. 1 – Variation of exciton binding energy as a function of dot radius of a ZnO/ $Zn_{1-x}Mg_xO$ quantum dot for different concentration of Mg with (line) and without (dashed curve) the internal field due to polarization effect

Fig. 3 shows the variation of second order nonlinear coefficient as a function of incident energy for a confined exciton for various dot radius of a ZnO/ $Zn_{0.8}Mg_{0.2}O$ quantum dot It is observed that the resonant peak is blue shifted as the dot radius decreases. It is because as ΔE increases as the dot radius decreases according to Eq. (22). The reason for the blue-shift is due to the higher transition energy when the dot radius is decreased. Further, we notice that the resonant rectification peak value is found to be linearly decreasing with the decrease in dot radius and the energy levels are separated largely with the reduction of overlap integral due to the increase in dipole matrix. It is because there occurs a competition between the energy interval and the dipole matrix element which determines these features.

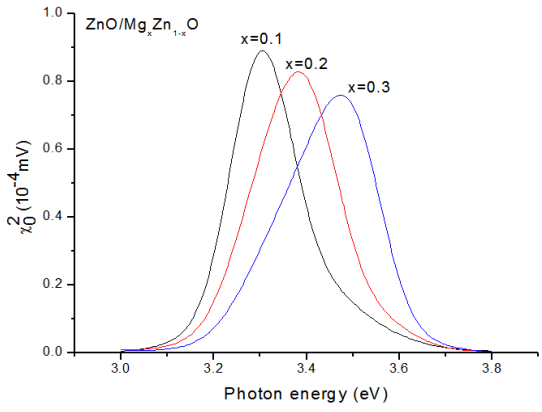

Fig. 2 – Variation of second order nonlinear coefficient as a function of incident energy for a confined exciton for various Mg alloy content in a 70 Å ZnO / $Zn_{1-x}Mg_xO$ quantum dot

Thus by decreasing the dot radius a remarkable blue-shift of the absorption resonant peak is induced, leading to a higher energy interval.

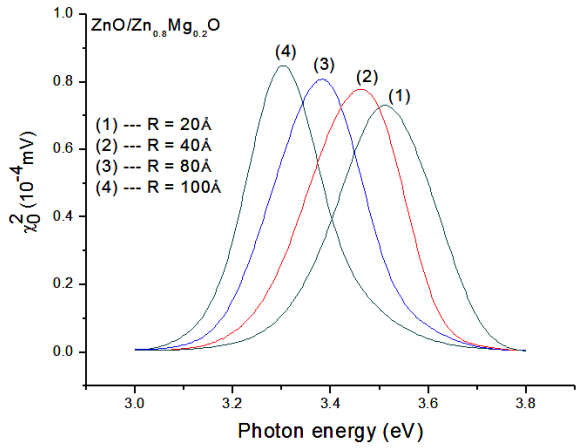

Fig. 3 – Variation of second order nonlinear coefficient as a function of incident energy for a confined exciton for various dot radius of a ZnO/ $Zn_{0.8}Mg_{0.2}O$ quantum dot

4. CONCLUSION

In the present paper, exciton binding energies of a heavy hole in a ZnO/$Mg_xZn_{1-x}O$ quantum dot have been investigated with the geometrical confinement and the Mg alloy content. The effects of strain, including the hydrostatic and the biaxial strain, and the internal electric field, including the spontaneous and piezoelectric polarization have been considered in all the calculations. Numerical calculations have been performed using variational procedure within the single band effective mass approximation. The nonlinear optical rectification as functions of dot radius and the values of Mg alloy content has been investigated in the strained ZnO/$Mg_xZn_{1-x}O$ quantum dot. A large value of nonlinear optical rectification has been obtained. Our results show that the nonlinear optical rectification is strongly dependent on the geometrical confinement and Mg alloy content. We believe that the results on the excitonic properties of Mg based II-VI semiconductor and the nonlinear optical properties would pave the way to find some optoelectronic phenomena experimentally.

ACKNOWLEDGEMENT

The author (AJP) thanks the CSIR, India for the grant (No.03 (1159)/10/EMR-II) for the financial support of this work.

REFERENCES

1. J. Han, M.H. Crawford, R.J. Shul, M. Banas, L. Zhang, Y.K. Song, H. Zhou, A.V. Nurmikko, *Appl. Phys. Lett.* **73**, 1688 (1998).
2. E. Monroy, M. Hamilton, D. Walker, P. Kung, F.J. Sanchez, M. Razeghi, *Appl. Phys. Lett.* **74**, 1171 (1999).
3. B.H. Kong, D.C. Kim, Y.Y. Kim, H.K. Cho, *J. Korean Phys. Soc.* **50**, 1701 (2007).
4. L.H. Ying, W.M. Yi, C.K. Jen, L.W. Jen, *IEEE J. Quantum Elect.* **20**, 2108 (2008).
5. S.H. Park, D. Ahn, *Appl. Phys. Lett.* **87**, 253509 (2005).
6. Y. Chen, D.M. Bagnall, H. Koh, K. Park, K. Hiraga, Z. Zhu, T. Yao, *J. Appl. Phys.* **84**, 3912 (1998).
7. M.-K. Wu, Y.-T. Shih, W.-C. Li, *IEEE J. Quantum Elect.* **20**, 1772 (2008).
8. R.T. Senger, K.K. Bajaj, *Phys. Rev. B* **68**, 205314 (2003). H.D. Sun, Makino, Y. Segawa, M. Kawasaki, A. Ohtomo, K. Tamura, H. Koinuma, *J. Appl. Phys.* **91**, 1993 (2002).
9. C. Morhain, T. Bretagnon, P. Lefebvre, X. Tang, P. Valvin, T. Guillet, B. Gil, T. Taliercio, M. Teisseire-Doninelli, B. Vinter, C. Deparis, *Phys. Rev. B* **72**, 241305 (2005).
10. J. Cui, *Appl. Phys. Lett.* **90**, 031905 (2007).
11. S.Y. Wei, L.L. Wei, C.X. Xia, X. Zhao, Y. Wang, *J. Lumin.* **128**, 1285 (2008).
12. Shuyi Wei, Qing Chang, Zaiping Zeng, *Cur. Appl. Phys.* **11**, 16 (2011).
13. B. Li, K.X. Guo, C.J. Zhang, Y.B. Zheng, *Phys. Lett. A* **367**, 493 (2007).
14. Q.H. Zhong, C.H. Liu, *Thin Solid Films* **516**, 3405 (2007).
15. I. Karabulut, H. Safak, M. Tomak, *Solid State Commun.* **135**, 735 (2005).
16. R.T. Senger, K.K. Bajaj, *Phys. Rev. B* **68**, 205314 (2003).
17. J. Singh, *Optoelectronics: An Introduction to Materials and Devices* (New Delhi: Tata McGraw Hill: 1996)
18. G.L. Bir, E. Pikus, *Symmetry and Strain-Induced Effects in Semiconductors* (New York: Wiley: 1974)
19. G. Coli, K.K. Bajaj, *Appl. Phys. Lett.* **78**, 2861 (2001).
20. P. Prete, N. Lovergine, L. Tapfer, A.M. Mancini, *Opt. Mat.* **17**, 207 (2001).
21. M. Yano et al., *JCG301-302* 353(2007).
22. F. Bernardini, V. Fiorentini, D. Vanderbilt, *Phys. Rev. Lett.* **79**, 3958 (1997).
23. P. Bigenwald, P. Lefebvre, T. Bretagnon, B. Gil, *Phys. Status Solidi B* **216**, 371 (1999).
24. S. Baskoutas, E. Paspalakis, A.F. Terzis, *Phys. Rev. B* **74**, 153306 (2006).
25. C.M. Duque, M.E. Mora-Ramos, C.A. Duque, *Superlattice. Microst.* **49**, 264 (2011).
26. W.-J. Fan, J.-B. Xia, P.-A. Agus, *J. Appl. Phys.* **99**, 013702 (2006).
27. T. Makino, Y. Segawa, M. Kawasaki, H. Koinuma, *Semicond. Sci. Technol.* **20**, S78 (2005).
28. Ansheng Liu, S.-L. Chuang, C.Z. Ning, *Appl. Phys. Lett.* **76**, 333 (2000).
29. Priya Gopal, Nicola A. Spaldin, *Phys Rev B*, **74**, 094418 (2004).
30. Anderson Janotti, Chris G. Van de Walle, *Phys. Rev. B* **75**, 121201 (2007).
31. J. Li, L. Liu, D. Yao, *Physica E* **27**, 221 (2005).